# Guided lock acquisition in a suspended Fabry–Perot cavity

**Jordan Camp, Lisa Sievers, Rolf Bork, and Jay Heefner**

*LIGO Project, California Institute of Technology, Pasadena, California 91125*

Received August 28, 1995

The process of lock acquisition in a high-finesse suspended Fabry–Perot cavity used in the LIGO 40-m interferometer is numerically simulated. The simulation, including a model of the cavity optical transient response as the mirrors swing through resonance, demonstrates that acquisition of lock by the controller depends on the relative velocity of the mirrors and establishes a threshold velocity below which acquisition may take place. The model results are used to implement a real-time controller that analyzes the transient response, extracts the mirror velocity, and then guides the mirrors into resonance with relative velocity under the threshold. The result is a factor-of-10 decrease in the experimentally observed acquisition time. © 1995 Optical Society of America

In its search for gravitational radiation from astrophysical sources, the Laser Interferometer Gravitational Wave Observatory (LIGO) will employ a Michelson interferometer with Fabry–Perot cavities in each arm.[1] The mirrors of the cavities are suspended for seismic isolation, to limit the contribution of thermal noise, and to allow low-noise control systems to maintain the correct cavity lengths and alignment. A servo control system will be used to hold the cavities in resonance with a high-power laser so that differential motion of the cavities, caused by a gravitational wave, can be measured. Length changes are observed by monitoring of the feedback that maintains resonance as the cavities are perturbed.

Servo operation takes place in the two different regimes of resonance and lock acquisition. When the servo is locked to the cavity resonance, the control-loop error signal shows a linear response to a change in cavity length; in contrast, the error signal has a highly nonlinear response to a cavity-length change as lock in being acquired. Although a servo design optimized for control on resonance is often used in both regimes, in practice it may not be effective at acquiring lock. At lower controller bandwidths, locking difficulties become pronounced, resulting in excessive down time associated with acquisition.

The LIGO 40-m interferometer,[2] consisting of two orthogonal 40-m Fabry–Perot cavities, serves as a test bed for the technology of the LIGO, including design and operation of its servoloops. The servos include a 1-MHz-bandwidth controller that stabilizes the laser frequency to one cavity and a 2-kHz controller that in turn stabilizes the other cavity to the light frequency through the positioning of a mirror. (The 2-kHz controller bandwidth is limited by the need to avoid excitation of mechanical resonances in the mirror.) In this Letter we report on a numerical model of the acquisition process in the 2-kHz-bandwidth controller and the implementation of a staged digital/analog controller based on the model results for dramatically improving the locking efficiency.

A block diagram of the position-controlled suspended high-finesse ($F \approx 15{,}000$) optical cavity is shown in Fig. 1. The magnetically actuated cavity is locked to frequency-stabilized laser light that is phase modulated in order to append radio-frequency (rf) sidebands to the carrier frequency.[3] The mirror position is controlled by a 2-kHz-bandwidth feedback system whose input is the demodulated photodiode signal and whose output is directed to a magnetic actuator.

The first step in the simulation of acquisition is to model the optical transient response of the cavity as it swings through resonance while illuminated by light of the carrier frequency. The procedure, depicted in Fig. 2, involves summing the amplitudes of all the light rays that propagate through the cavity and return to the input mirror at times that are integral multiples of the round-trip light travel time $\tau = 2L/c$. The electric-field amplitude of the $i$th ray is given by $E_i = (r_1 r_2)^i [\exp(jkL_i)]$, where $r_1$ and $r_2$ are the amplitude reflectivities of the input and the end mirrors, $k$ is the carrier wave number, and $L_i$ is the total path traveled for the $i$th ray (taking into account the changing cavity length). The rays at any time include light newly entered and reflected light stored for many round trips inside the high-finesse cavity. The optical transient is obtained from the interference of the reflected rf sidebands (nonresonant in the cavity) with the light leaking out of the cavity, which is then demodulated with the local rf reference. The resultant signal is proportional to $\mathrm{Im}(\sum E_i)$, the imaginary part of the cavity field at the input mirror. The oscillatory shape of the signal, simulated for a relative mirror velocity of 1 $\mu$m/s in Fig. 2(b), may be interpreted as being caused by beating of the older rays of relatively larger Doppler shift with the more recent rays propagating through the cavity.

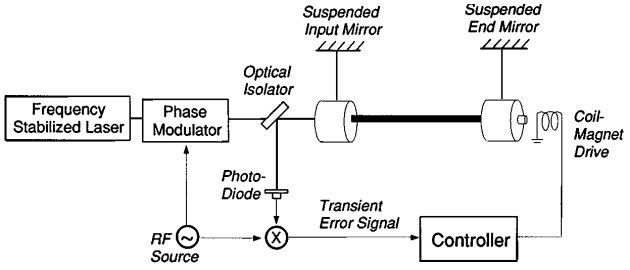


Fig. 1. Feedback configuration used to control the 40-m cavity length.

0146-9592/95/242463-03$6.00/0 

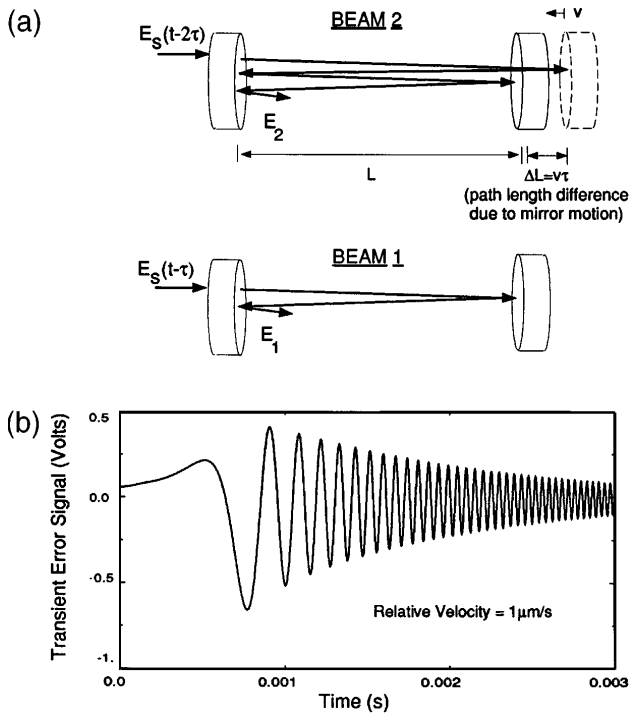


Fig. 2. Illustration of the optical response model: (a) First two beams used in sum to calculate the cavity electric field at time $t$. The $i$th beam enters the cavity at time $(t - i\tau)$, where $\tau = 2L/c$. The mirror motion affects the path length. (b) Simulated transient error signal for a relative velocity of 1 $\mu$m/s.

The next step is the numerical integration of the set of differential equations that describes the servo response to the transient error signal. The need for both computation speed and stability (given the presence of saturating electronic levels) led to the choice of fourth-order Runge–Kutta equations. This technique reduces the $N$ servo gain stages and filters (including the pendulum response of the suspended mirror) to a set of $N$ coupled first-order differential equations. Saturation of photodiode and amplifiers, independently measured, is included. The integration over the (adaptive) step size d$t$ (taken as an integral multiple of $\tau$) advances the mirror at a constant velocity to a new position, at which point the ray propagation over the interval d$t$ is performed.

The simulated phase-plane plots shown in Fig. 3 identify the maximum relative mirror velocity for which the analog servo will acquire lock (the threshold velocity). In the first trace the mirror velocity is low enough that the servo acquires lock in the first encounter with the cavity resonant length. In the second case the velocity is higher and the mirror swings past the resonance but is slowed sufficiently so that it returns and is caught. In the final case the velocity is so high that the servo has little effect and the mirror swings past. The crucial parameter that establishes the threshold velocity is the servo bandwidth: the servo response time must be sufficiently short to follow the oscillating transient error signal [Fig. 2(b)] to have an effect on the mirror velocity. As the velocity is raised above threshold, the oscillation frequency increases and the servo can no longer respond to the input. For the 2-kHz bandwidth of the analog controller we find a threshold velocity of $\sim$0.2 $\mu$m/s, lowered to $\sim$0.15 $\mu$m/s by the presence of electronic saturation.

In the current LIGO 40-m interferometer, seismic motion drives the suspended mirrors with an average relative velocity of $\sim$1 $\mu$m/s, seven times the threshold. To address this problem, we incorporate a real-time digital controller to determine the relative mirror velocity through the cavity transient response and then apply a current pulse to the coil to guide the mirrors into resonance with a velocity under the threshold, so that the original analog servo may be used effectively. A block diagram of the controller is shown in Fig. 4. A relay divides the operation into digital and analog regimes. The initial state is digital. A trigger signal is obtained from the photodiode dc output, which discriminates in favor of a carrier resonance as opposed to that of a sideband. The trigger gates the analog-to-digital converter, which digitizes the transient signal over a 1.5-ms interval with a sampling rate of 100 kHz. We obtain the relative mirror speed by measuring the time between zero crossings of the digitized waveform and using a fitted function derived from the model to relate velocity to crossing time. The sign of the initial peak in the waveform gives the mirror direction. A current pulse is then sent to the coil ($\sim$2.5 ms after the trigger), resulting in an impulse that reverses the mirror direction and brings it back to the resonance with lowered relative velocity. (The impulse is derived

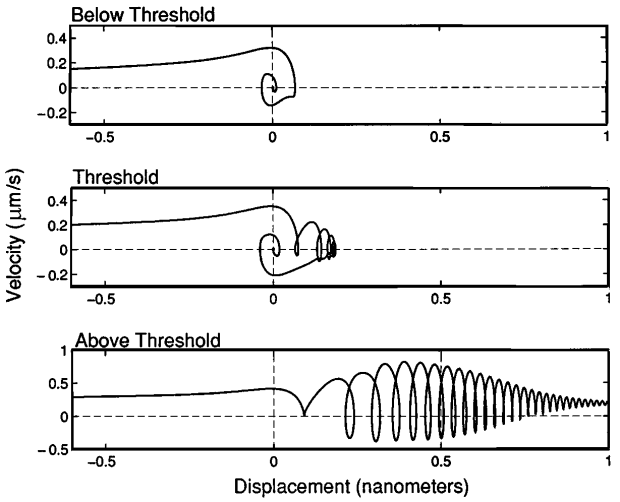


Fig. 3. Phase-plane plots showing trajectories for three different initial velocities approaching resonance: below threshold, threshold, and above threshold.

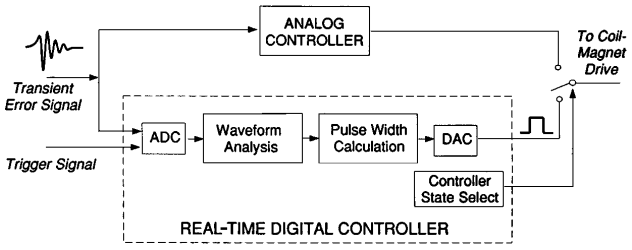


Fig. 4. Block diagram of the staged digital/analog controller. ADC, analog-to-digital converter; DAC, digital-to-analog converter.

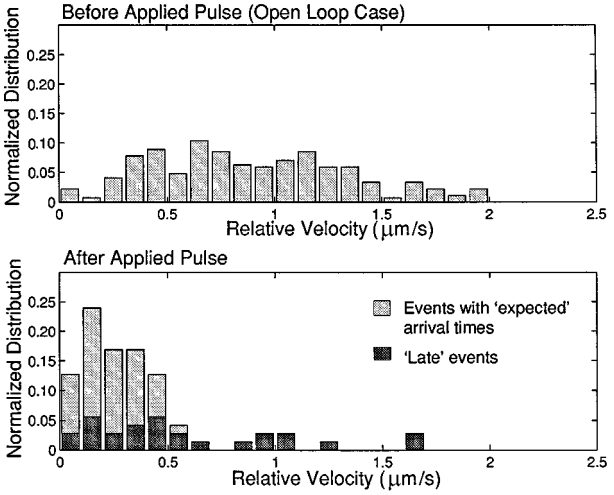


Fig. 5. Measured velocity distribution before the applied pulse (as the cavity first approaches resonance) and after the applied pulse (as the cavity returns to the resonance condition).

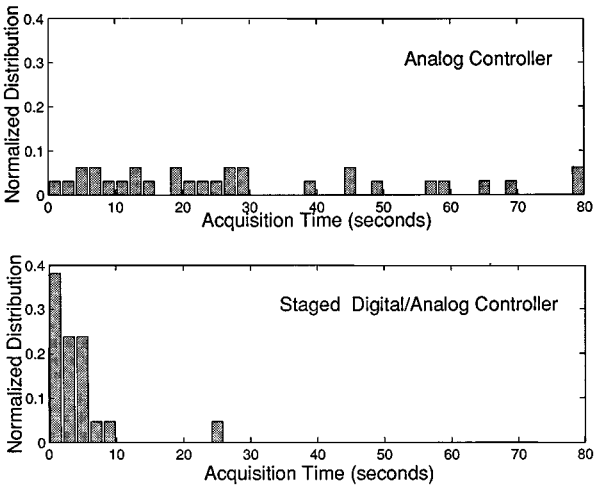


Fig. 6. Comparison of experimental acquisition time with analog and staged digital/analog controllers.

only from the relative motion of the mirrors and in fact causes the actuated mirror to follow the other.) The mechanical relay then activates the analog servo. In the event that the analog servo does not lock, the process is repeated.

In Fig. 5 we show the effect of the digital-controller impulse on the velocity distribution of the mirror passing through cavity resonance. The impulse for each event was calculated to bring the mirror back to the resonance with a velocity of 0.1 $\mu$m/s. The upper plot shows the velocity distribution of the mirror with no feedback, and the lower plot shows the velocity distribution obtained with the use of the digital controller. As the mirror guidance takes place amid a background of seismic excitation (the dominant modes are the pendulum suspension at 1 Hz and a resonance of the vibration isolation platform at 3 Hz), the return velocity and the arrival time are found to be distributed about the calculated values. The corrupting effect of seismic noise is also seen in the flat distribution of late events (those with arrival times greater than twice the kinematically expected time). The width of the return velocity distribution was found to be correlated with the calculated return velocity: a lower return velocity takes longer to return to the resonance and is more likely to be corrupted by seismic motion.

An optimal calculated return velocity for lock acquisition is thus expected to be just under threshold, as this minimizes the time that the mirror spends in returning to the resonance. We found empirically the best performance for a calculated return velocity of 20% of the input velocity. Figure 6 shows the comparison of acquisition times for the analog and the staged digital/analog controller. We find the average time to acquire lock to be ~4 s in the staged-controller mode, compared with 35 s for the analog. The lower limit may be influenced by instability in the analog servo during acquisition: events below threshold were observed that triggered a servo instability and did not result in acquisition.

In summary, we have reported on a real-time analysis of the optical transient response of a suspended Fabry–Perot cavity to guide its acquisition of lock. The goal of implementing guided lock acquisition for the LIGO interferometer (which includes a recycling mirror that couples the arm cavities) will require the formulation of an accurate optical response model and an analysis/simulation of the best strategy for locking multiple cavities in the presence of seismic excitation.

We thank our colleagues on the LIGO project for their support. We thank M. Regehr and D. Redding for helpful discussions on earlier work on Fabry–Perot optical modeling. Matlab software, donated to the LIGO project by The Math Works, Inc., was used in the servo modeling and design. This work is supported by the National Science Foundation under Cooperative Agreement PHY-9210038.

## References

1. A. Abramovici, W. Althouse, R. Drever, Y. Gursel, S. Kawamura, F. J. Raab, D. Shoemaker, L. Sievers, R. Spero, K. Thorne, R. Vogt, R. Weiss, S. Whitcomb, and M. Zucker, Science **256,** 325 (1992).
2. A. Abramovici, W. Althouse, J. Camp, D. Durance, J. Giaime, A. Gillespie, S. Kawamura, A. Kuhnert, T. Lyons, F. J. Raab, R. L. Savage, Jr., D. Shoemaker, L. Sievers, R. Spero, R. Vogt, R. Weiss, S. Whitcomb, and M. Zucker, "Improved sensitivity in the LIGO 40-meter interferometer," submitted to Science.
3. R. W. P. Drever, J. L. Hall, F. V. Kowalski, J. Hough, G. M. Ford, A. J. Munley, and H. Ward, Appl. Phys. B **31,** 97 (1983).